Supporting information

For

Luminescent and Proton Conducting Lanthanide Coordination Networks Based on a Zwitterionic Tripodal Triphosphonate

Montse Bazaga-García,[†] Giasemi K. Angeli,[¥] Konstantinos E. Papathanasiou,[¥] Inés R. Salcedo,[†] Pascual Olivera-Pastor,[†] Enrique R. Losilla,[†] Duane Choquesillo-Lazarte,[§] Gary B. Hix,[‡] Aurelio Cabeza,[†,] and Konstantinos D. Demadis,*[¥]*

[¥]Crystal Engineering, Growth and Design Laboratory, Department of Chemistry, University of Crete, Voutes Campus, Crete, GR-71003, Greece

[†]Universidad de Málaga, Departamento de Química Inorgánica, Campus Teatinos s/n 29071-Málaga, Spain

[§]Laboratorio de Estudios Cristalográficos, IACT-CSIC, Granada, Spain

[‡]School of Science and Technology, Nottingham Trent University, Clifton Lane, Nottingham, NG11 8NS, United Kingdom

TABLE OF CONTENTS:

Figures:

S21. UV-visible absorption spectrum for Ho-H_4NMPCl.

Tables:

S1. Selected bond distances (Å) for Ln-H_4NMPCl, (Ln= La, Pr, Sm, Eu, Gd, Tb, Dy and Ho) and Ce-H_3NMP.

S2. H-bond interactions (Å) for $[Ce_2(H_3NMP)_2(H_2O)_4]\cdot 4.5H_2O$.

S3. Absorption and emission bands observed for $[Pr(H_4NMP)(H_2O)_2]Cl\cdot 2H_2O$.

S4. Absorption and emission bands observed for $[Sm(H_4NMP)(H_2O)_2]Cl\cdot 2H_2O$.

S5. Absorption and Emission bands observed for $[Eu(H_4NMP)(H_2O)_2]Cl\cdot 2H_2O$.

S6. Absorption and emission bands observed for $[Tb(H_4NMP)(H_2O)_2]Cl\cdot 2H_2O$.

S7. Absorption and emission bands observed for $[Dy(H_4NMP)(H_2O)_2]Cl\cdot 2H_2O$.

S8. Absorption and emission bands observed for $[Ho(H_4NMP)(H_2O)_2]Cl\cdot 2H_2O$.

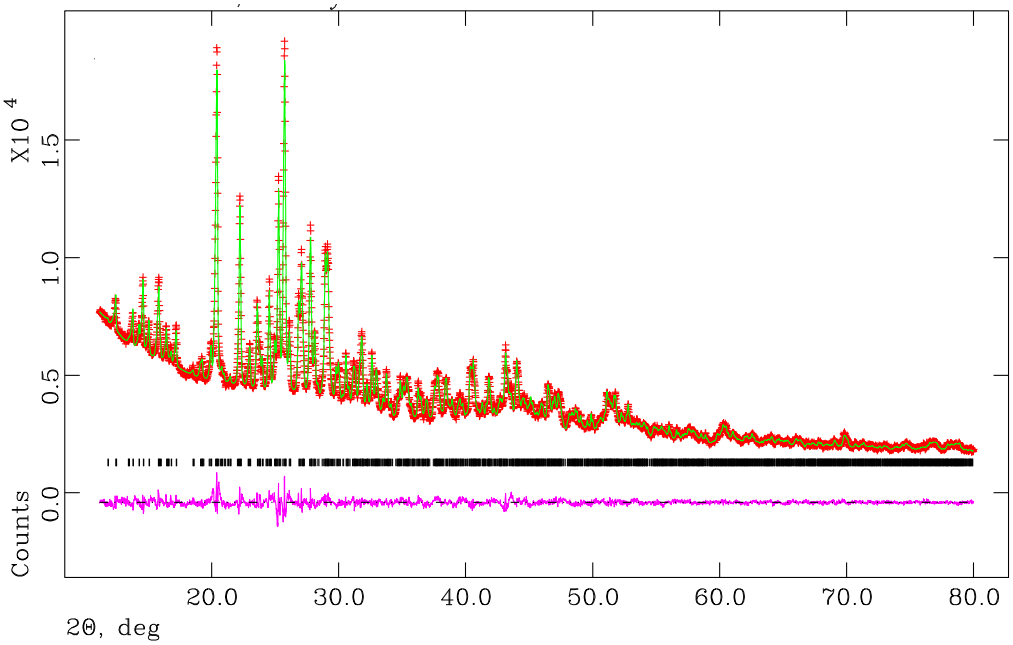

Figure S1. Rietveld plot for **$[Ce_2(H_3NMP)_2(H_2O)_4]\cdot 4.5H_2O$**. Experimental data (red scatters); the best-fit profile (upper trace) and the difference pattern (lower trace) are drawn as solid green and magenta lines, respectively. Black vertical bars indicate the angular positions of the allowed Bragg reflections.

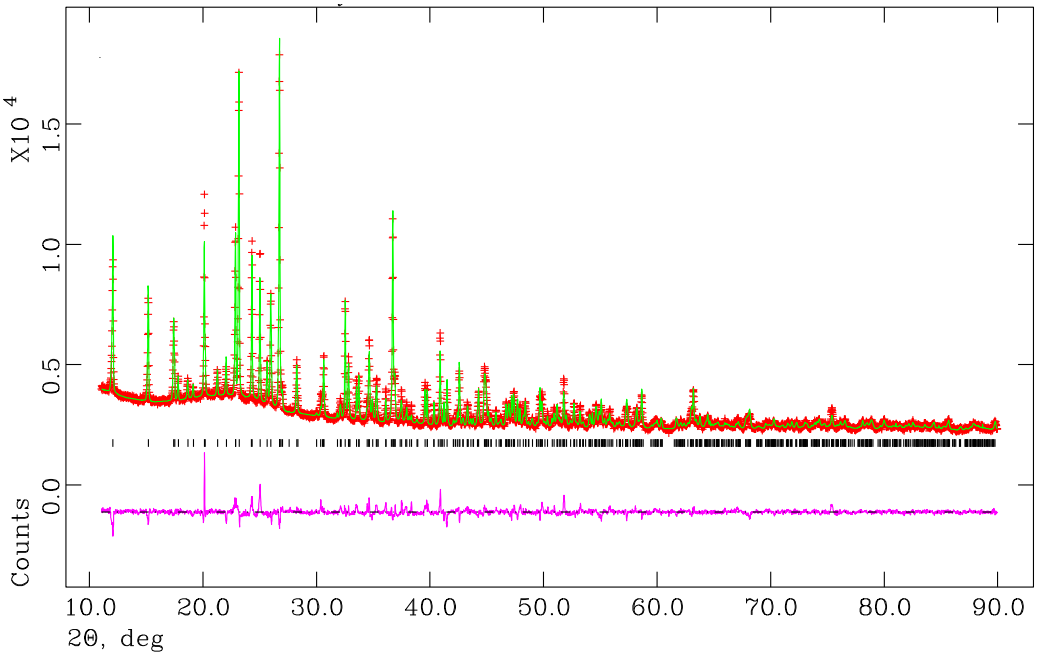

Figure S2. Rietveld plot for **$[Sm(H_4NMP)(H_2O)_2]Cl\cdot 2H_2O$**. Experimental data (red scatters); the best-fit profile (upper trace) and the difference pattern (lower trace) are drawn as solid green and magenta lines, respectively. Black vertical bars indicate the angular positions of the allowed Bragg reflections.

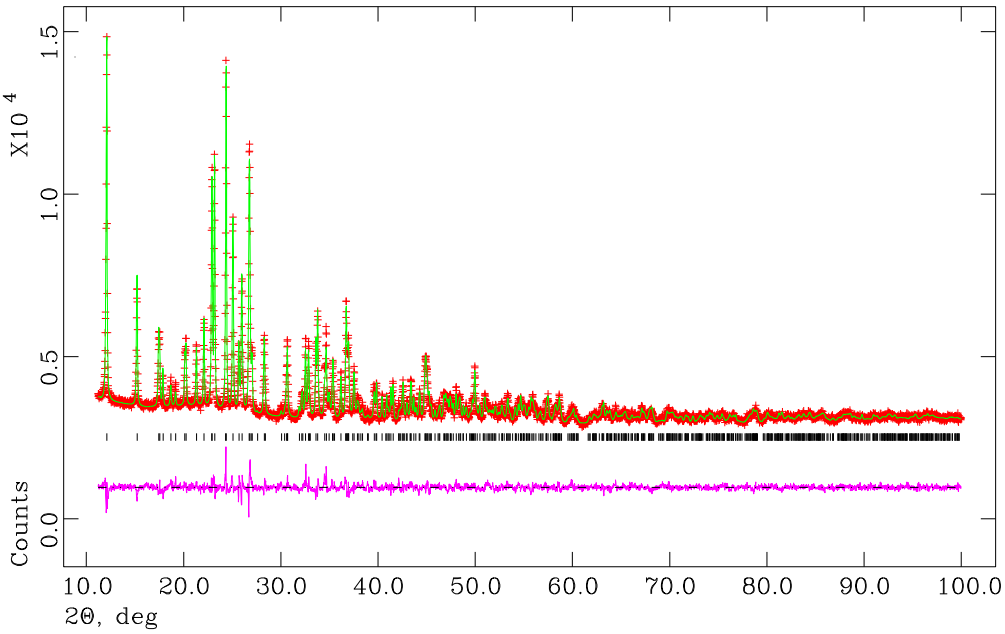

Figure S3. Rietveld plot for **[Eu(H$_4$NMP)(H$_2$O)$_2$]Cl·2H$_2$O** Experimental data (red scatters); the best-fit profile (upper trace) and the difference pattern (lower trace) are drawn as solid green and magenta lines, respectively. Black vertical bars indicate the angular positions of the allowed Bragg reflections.

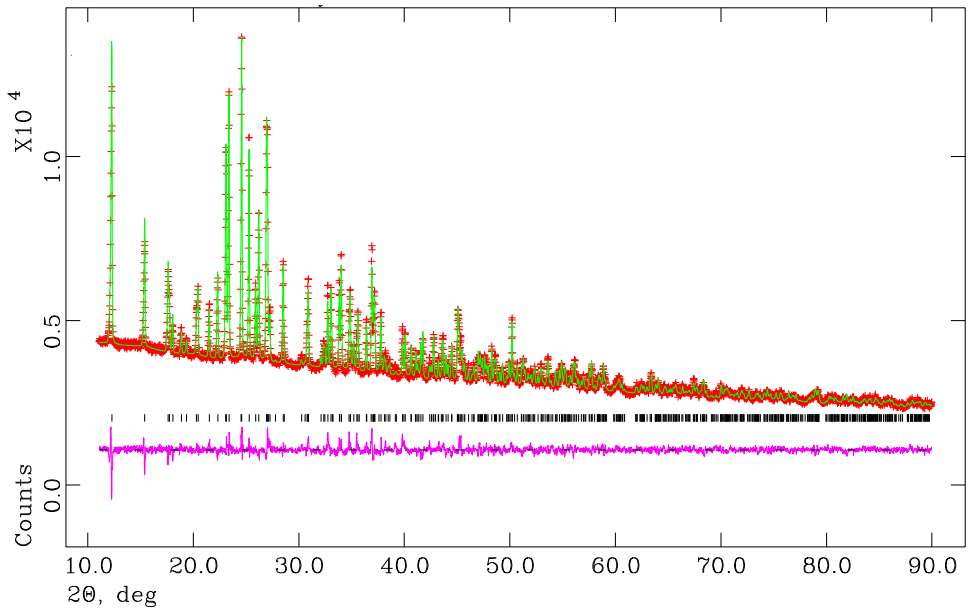

Figure S4. Rietveld plot for **[Gd(H$_4$NMP)(H$_2$O)$_2$]Cl·2H$_2$O** Experimental data (red scatters); the best-fit profile (upper trace) and the difference pattern (lower trace) are drawn as solid green and magenta lines, respectively. Black vertical bars indicate the angular positions of the allowed Bragg reflections.

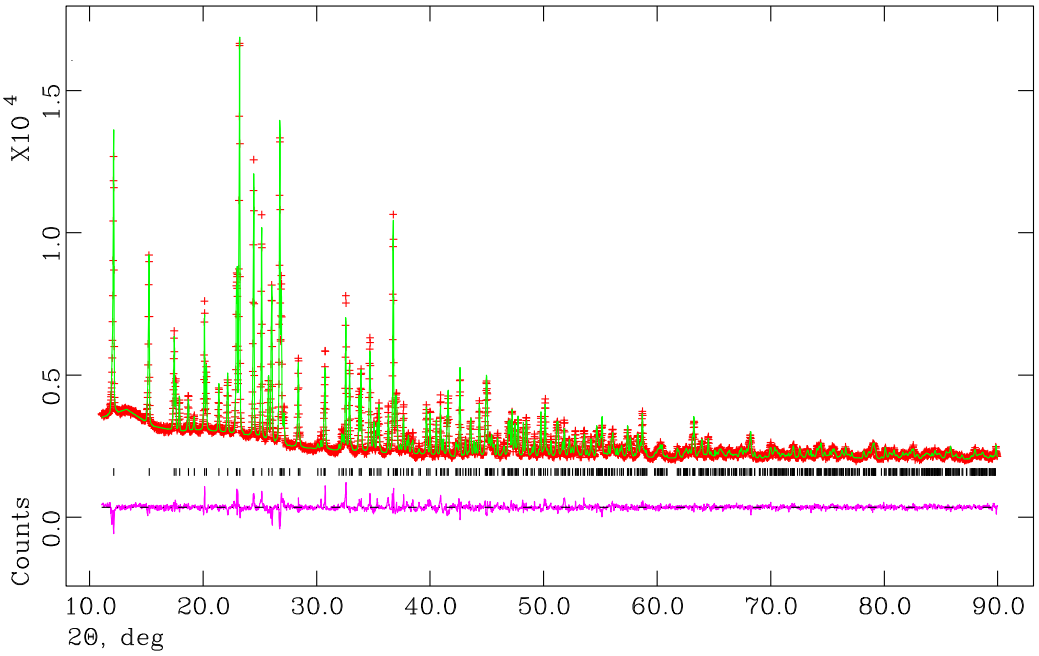

Figure S5. Rietveld plot for **[Tb(H$_4$NMP)(H$_2$O)$_2$]Cl·2H$_2$O** Experimental data (red scatters); the best-fit profile (upper trace) and the difference pattern (lower trace) are drawn as solid green and magenta lines, respectively. Black vertical bars indicate the angular positions of the allowed Bragg reflections.

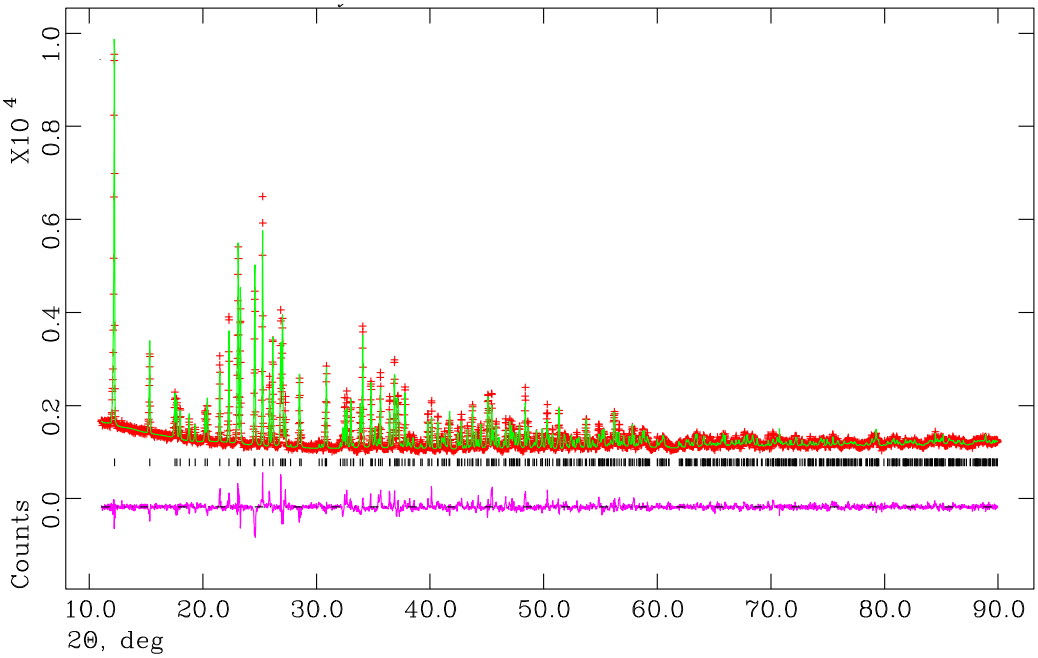

Figure S6. Rietveld plot for **[Dy(H$_4$NMP)(H$_2$O)$_2$]Cl·2H$_2$O**. Experimental data (red scatters); the best-fit profile (upper trace) and the difference pattern (lower trace) are drawn as solid green and magenta lines, respectively. Black vertical bars indicate the angular positions of the allowed Bragg reflections.

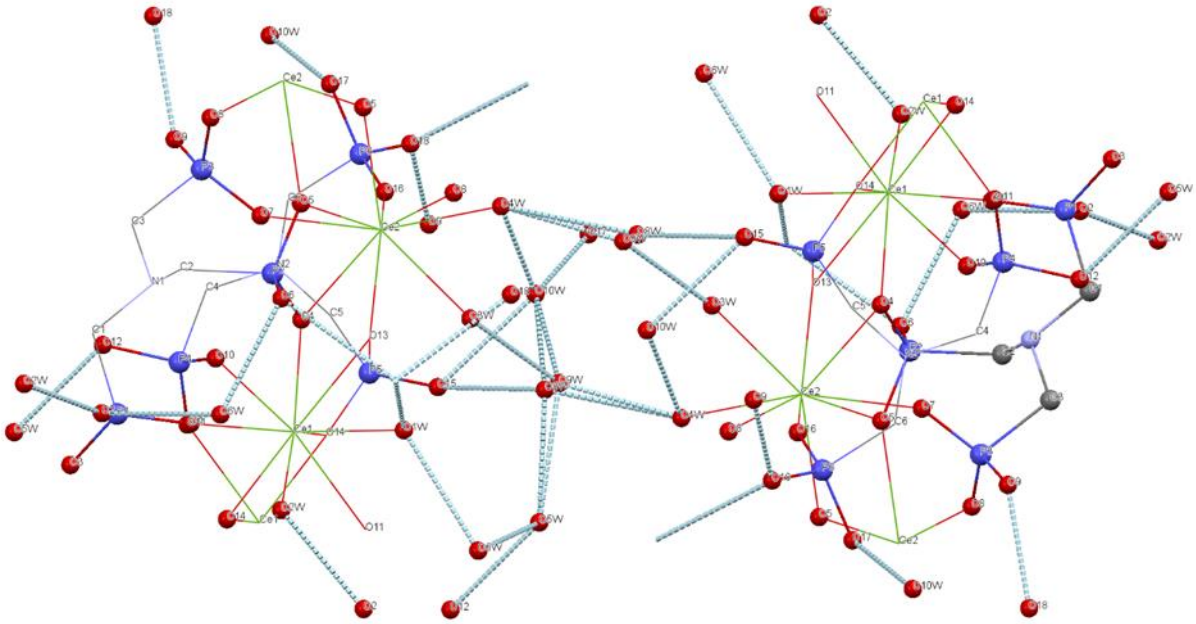

Figure S7. Extended hydrogen bonding interactions observed in the crystal structure of **$[Ce_2(H_3NMP)_2(H_2O)_4]\cdot 4.5H_2O$**.

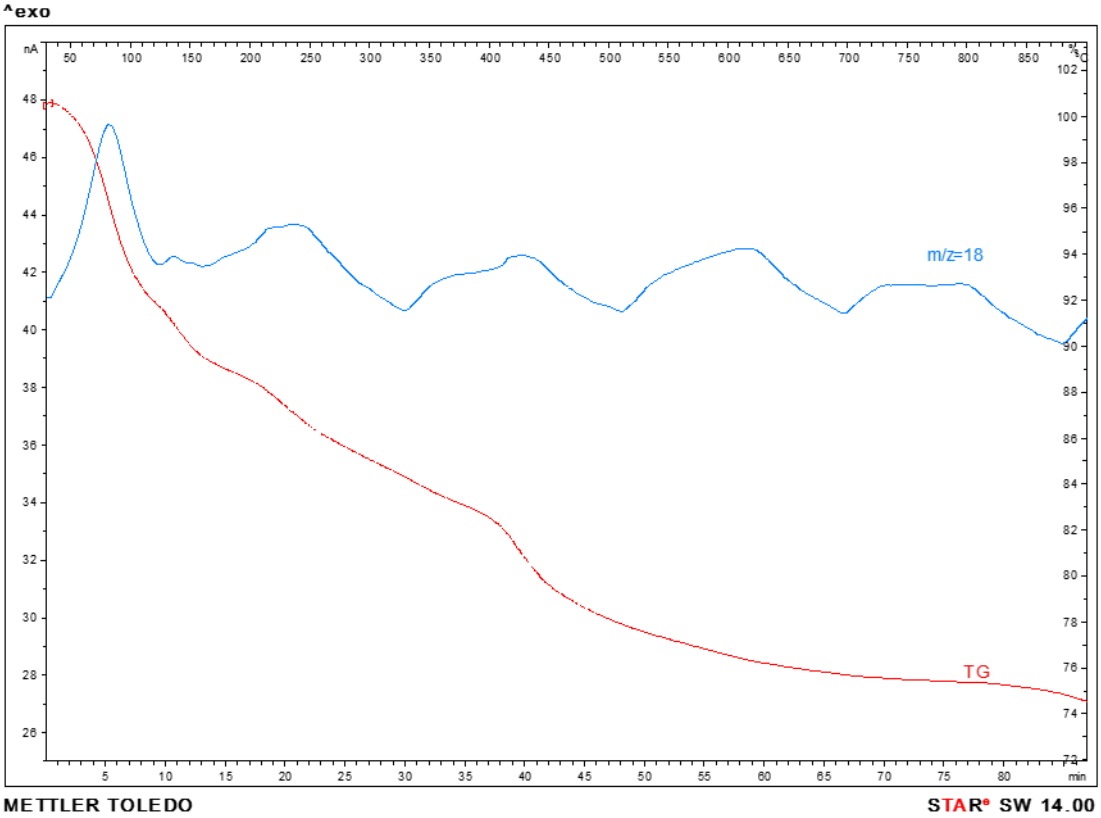

Figure S8. TG-MS curves for **[Gd(H$_4$NMP)(H$_2$O)$_2$]Cl·2H$_2$O** and H$_2$O (m/z = 18).

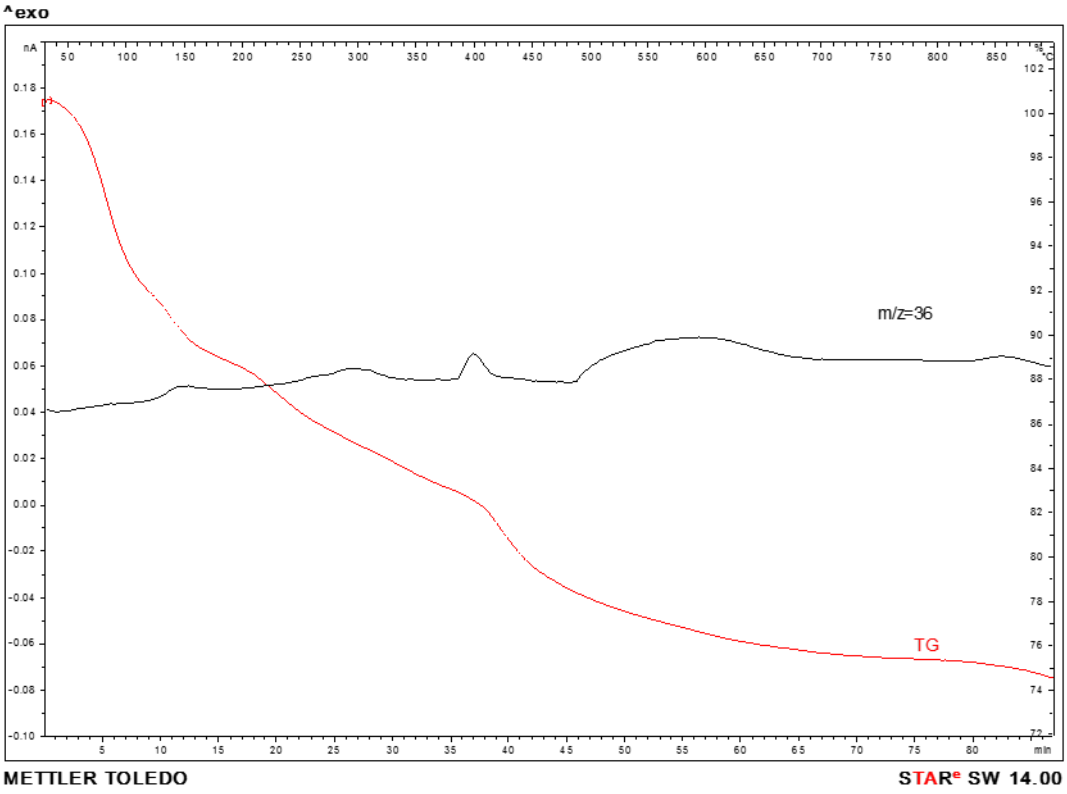

Figure S9. TG-MS curves for **[Gd(H$_4$NMP)(H$_2$O)$_2$]Cl·2H$_2$O** and HCl (m/z = 36).

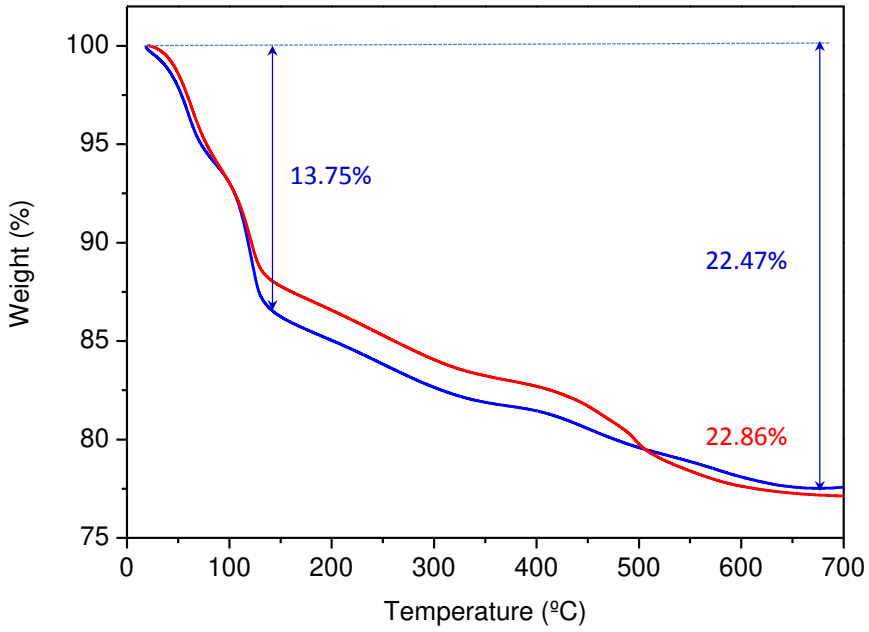

Figure S10. TGA curves for **$[Ce_2(H_3NM)_2(H_2O)_4]\cdot 4.5H_2O$** as-synthesized (blue) and post-impedance analysis (red).

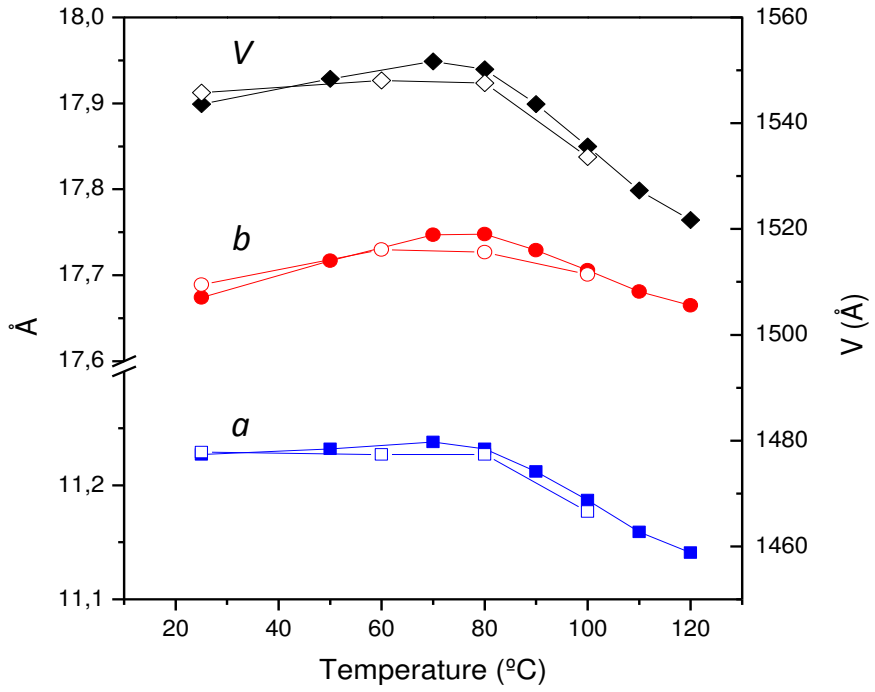

Figure S11. Variation of unit cell parameters and volume with the temperature for **$[Sm(H_4NMP)(H_2O)_2]Cl\cdot 2H_2O$** (open and filled symbols denote decreasing and increasing temperatures, respectively).

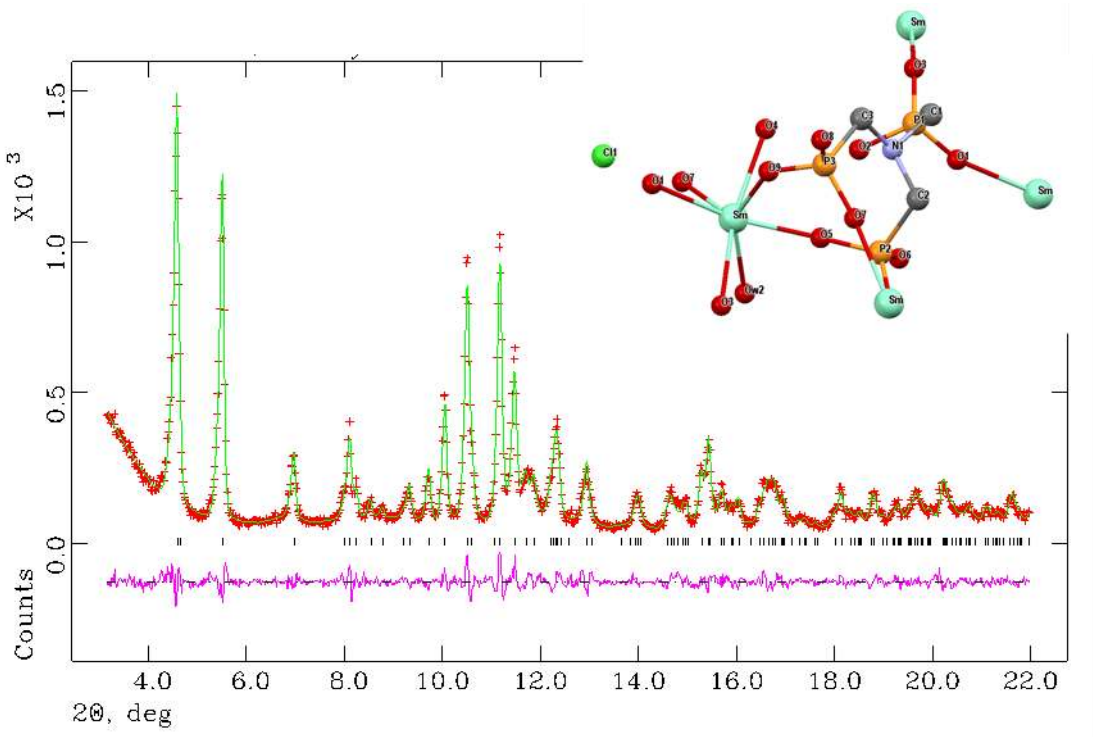

Figures S12. Rietveld plot of **[Sm(H$_4$NMP)(H$_2$O)]Cl** heated at 120 °C and 10% RH. The powder pattern was collected using Mo $K_{\alpha 1}$ radiation (λ= 0.7093 Å). The inset shows the coordination environment around Sm^{3+} in **[Sm(H$_4$NMP)(H$_2$O)]Cl**. Selected crystallographic data: a= 11.142(2) Å; b= 17.653(4) Å; c= 8.610(1) Å; β= 116.135(8)° ; V= 1520.4(7) Å^3; s.g. *C c*; R_{WP}= 0.0872; R_P= 0.0678; R_F= 0.0151.

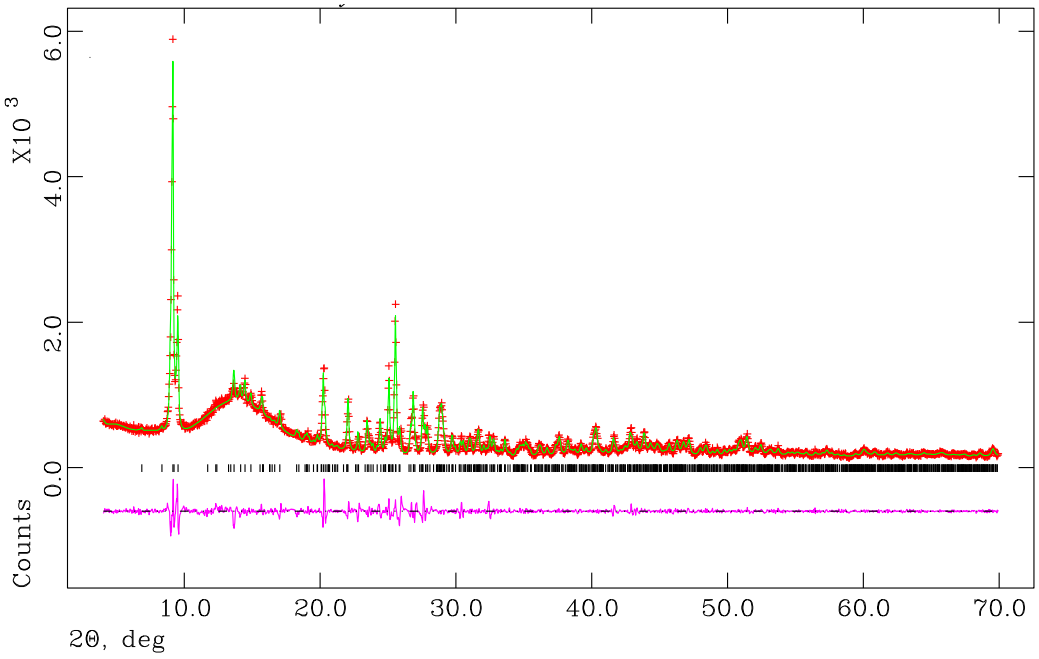

Figure S13. Le Bail fit for **[La$_2$(H$_3$NMP)$_2$(H$_2$O)$_4$]·4.5H$_2$O** obtained by exposing [La(H$_4$NMP)(H$_2$O)$_2$]Cl·2H$_2$O at 80 ºC and 95% RH for 30 h.

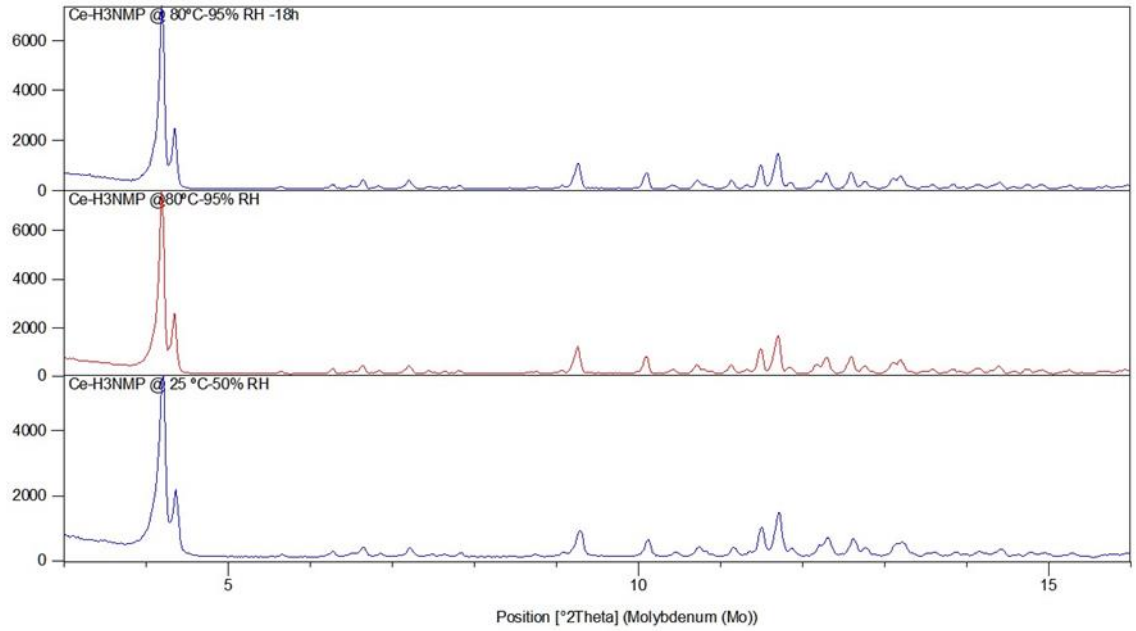

Figure S14. Powder XRD patterns for **$[Ce_2(H_3NMP)_2(H_2O)_4]\cdot 4.5H_2O$** at: (a) 25 °C and 50% RH; (b) 80 °C and 95% RH after 1 h; and (c) 80 °C and 95 % RH after 18 h.

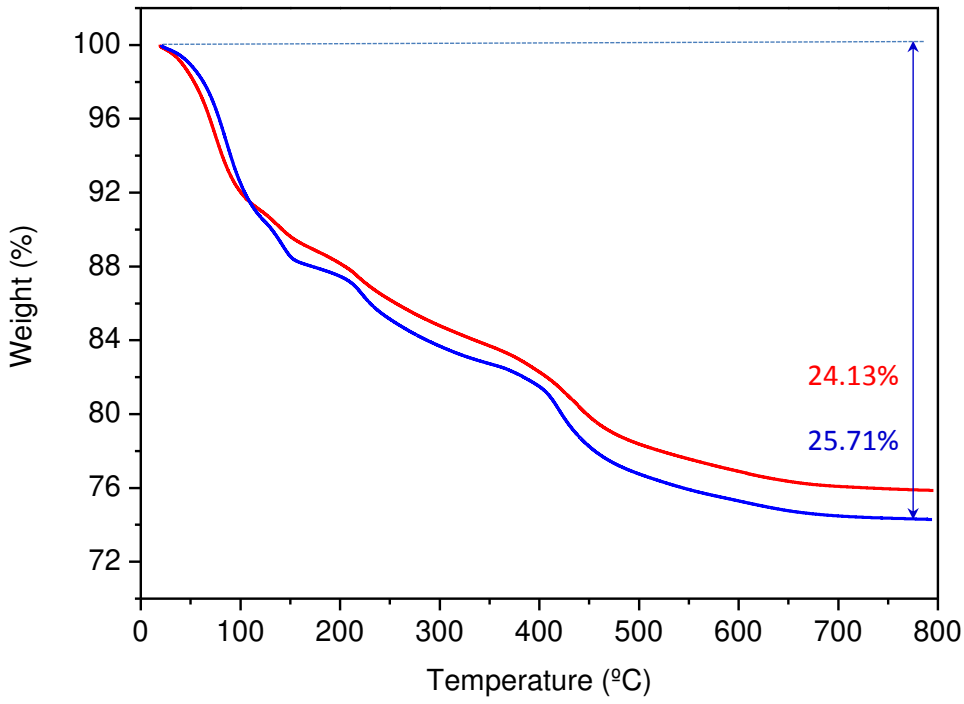

Figure S15. TGA curves of **$[Gd(H_4NMP)(H_2O)_2]Cl\cdot 2H_2O$** as-synthesized (blue) and post-impedance (red).

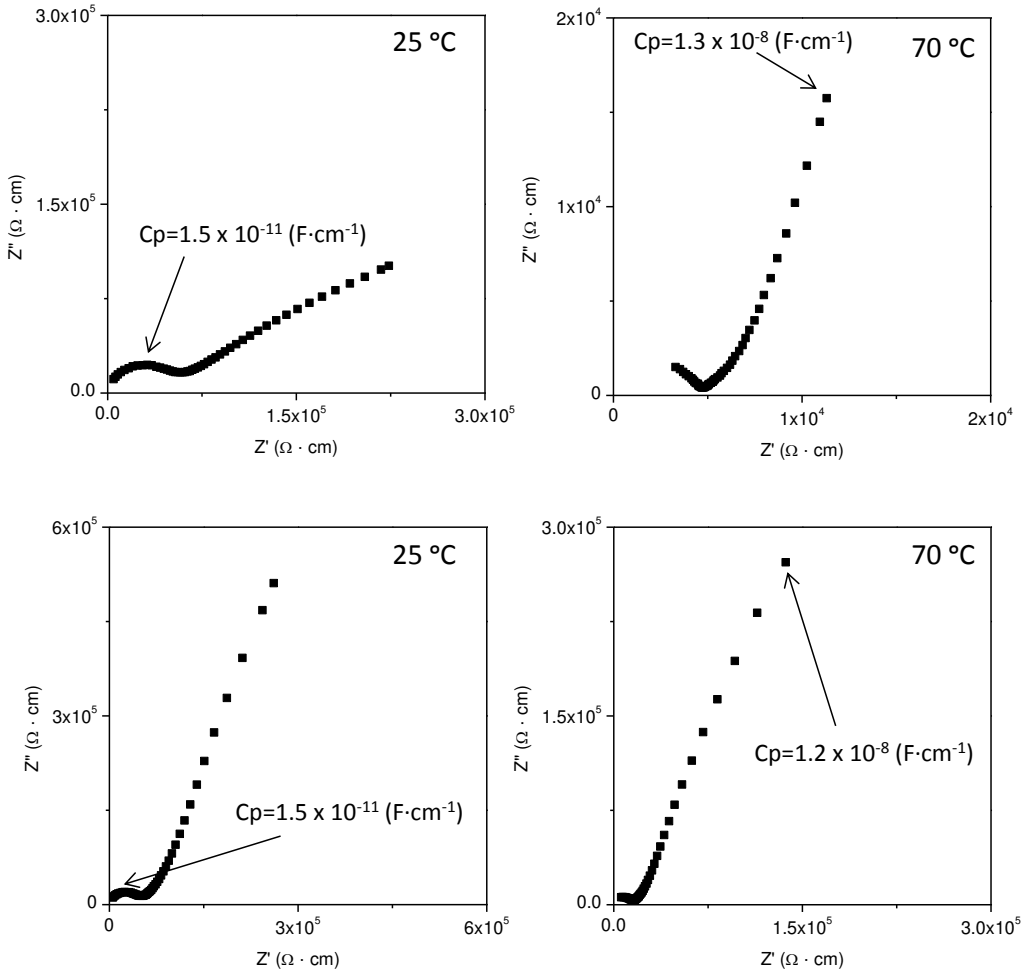

Figure S16. Complex impedance plane plots at 25 and 70 ºC (95% RH) for (a) **[Gd(H$_4$NMP)(H$_2$O)$_2$]Cl·2H$_2$O** and (b) **[Ce$_2$(H$_3$NMP)$_2$(H$_2$O)$_4$]·4.5H$_2$O**.

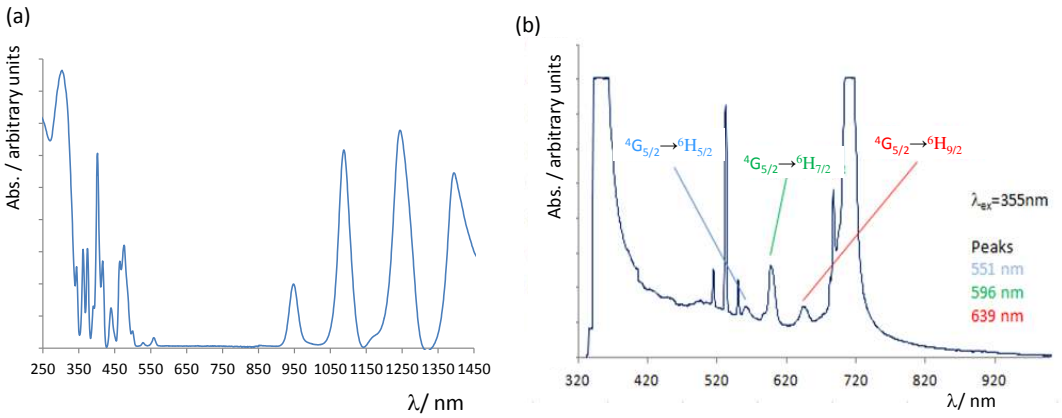

Figure S17. (a) UV-visible absorption and (b) emission spectra for **Sm-H$_4$NMPCl**.

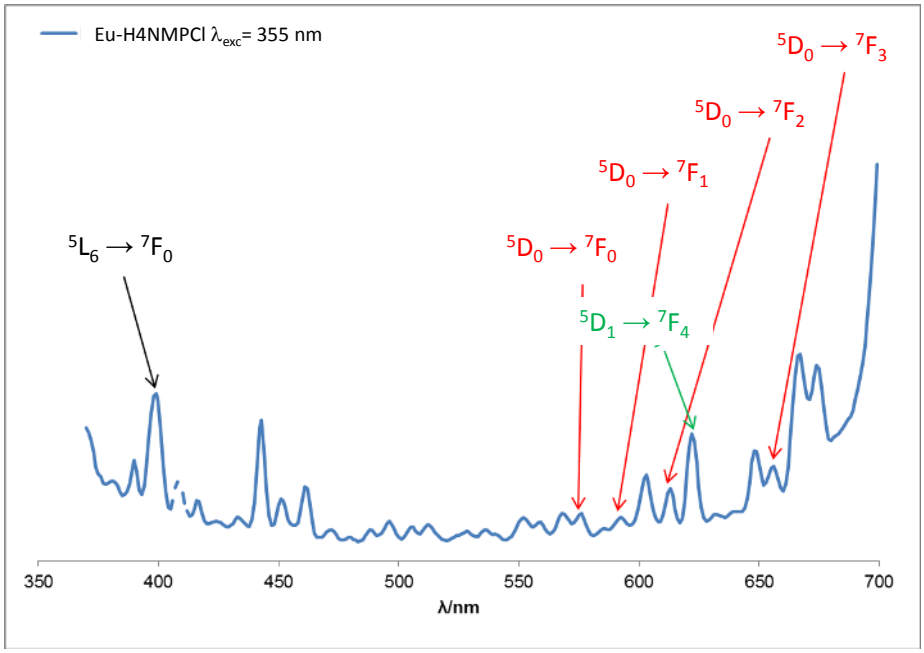

Figure S18. Emission spectrum for **Eu-H$_4$NMPCl**.

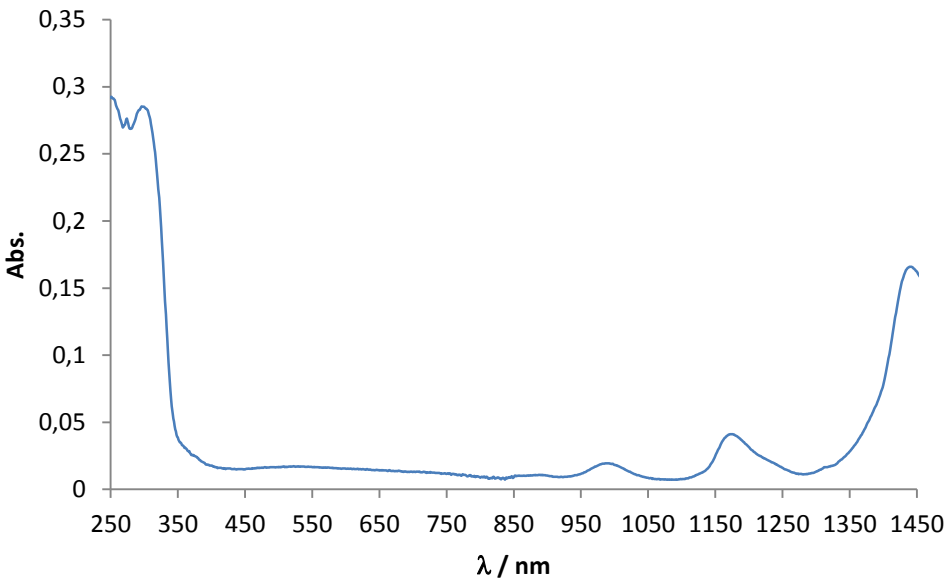

Figure S19. UV-visible absorption spectrum for **Gd-H_4NMPCl**.

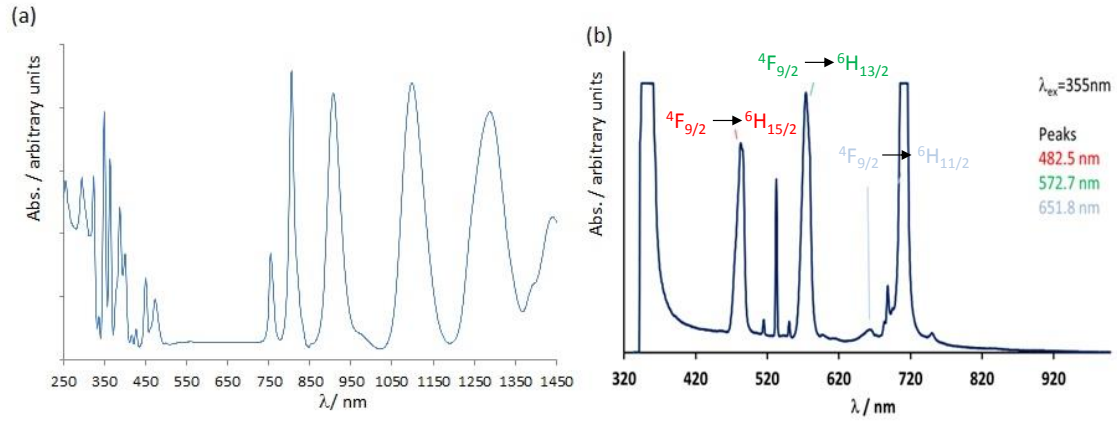

Figure S20. (a) UV-visible absorption and (b) emission spectra for **Dy-H_4NMPCl**.

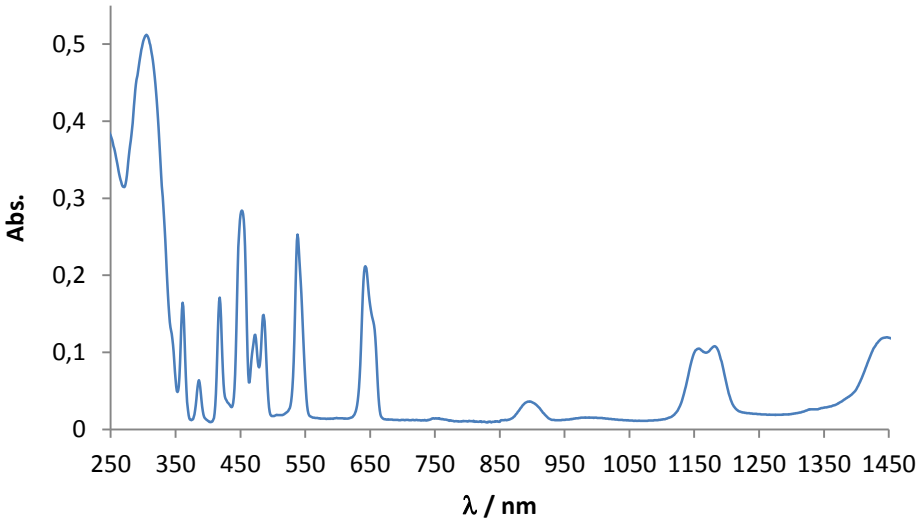

Figure S21. UV-visible absorption spectrum for **Ho-H_4NMPCl**.

Table S1. Selected bond distances (Å) for **Ln-H_4NMPCl**, (Ln= La, Pr, Sm, Eu, Gd, Tb, Dy and Ho) and **Ce-H_3NMP**.

[La(H_4NMP)(H_2O)$_2$]Cl·2H_2O					
	Length (Å)		**Length (Å)**		**Length (Å)**
La1-O8	2.439(2)	P2-O10	1.497(3)	P4-O13	1.497(2)
La1-O20	2.458(2)	P2-O19	1.509(2)	P4-O11	1.497(2)
La1-O10	2.466(3)	P2-O24	1.589(2)	P4-O12	1.583(3)
La1- O19	2.470(2)	P2-C17	1.823(4)	P4-C18	1.839(3)
La1-O11	2.485(2)	P3-O20	1.496(2)	N9-C18	1.508(4)
La1-O13	2.487(2)	P3-O8	1.496(2)	N9-C17	1.508(4)
La1-O14	2.559(3)	P3-O15	1.570(3)	N9-C22	1.525(4)
La1-O6	2.649(3)	P3-C22	1.829(3)		
[Ce_2(H_3NMP)$_2$(H_2O)$_4$]·4.5H_2O					
	Length (Å)		**Length (Å)**		**Length (Å)**
Ce1-O1w	2.608(3)	P1-O1	1.526(4)	P5-O13	1.538(4)
Ce1-O2w	2.832(3)	P1-O2	1.533(4)	P5-O14	1.545(4)
Ce1-O1	2.306(1)	P1-O3	1.535(4)	P5-O15	1.539(4)
Ce1-O4	2.489(2)	P1-C1	1.800(4)	P5-C5	1.810(4)
Ce1-O10	2.469(2)	P2-O4	1.539(4)	P6-O16	1.545(4)
Ce1-O11	2.398(2)	P2-O5	1.543(4)	P6-O17	1.538(4)
Ce1-O13	2.943(2)	P2-O6	1.546(4)	P6-O18	1.542(4)
Ce1-O14	2.677(2)	P2-C2	1.808(4)	P6-C6	1.804(4)
Ce1-O14	2.545(1)	P3-O7	1.540(4)	N1-C1	1.507(4)
Ce2-O3w	2.484(3)	P3-O8	1.533(4)	N1-C2	1.494(4)
Ce2-O4w	2.427(3)	P3-O9	1.540(4)	N1-C3	1.507(4)
Ce2-O4	2.713(2)	P3-C3	1.807(4)	N2-C4	1.503(4)
Ce2-O5	2.729(2)	P4-O10	1.535(4)	N2-C5	1.501(5)
Ce2-O5	2.374(2)	P4-O11	1.535(4)	N2-C6	1.509(4)
Ce2-O7	2.497(2)	P4-O12	1.548(4)		
Ce2-O8	2.363(2)	P4-C4	1.805(4)		
Ce2-O13	2.404(1)				
Ce2-O16	2.440(1)				
[Pr(H_4NMP)(H_2O)$_2$]Cl·2H_2O					
	Length (Å)		**Length (Å)**		**Length (Å)**
Pr1-O8	2.395(8)	P2-O19	1.495(9)	P4-O13	1.484(9)
Pr1-O20	2.407(9)	P2-O10	1.506(11)	P4-O11	1.494(9)
Pr1-O10	2.426(1)	P2-O24	1.585(9)	P4-O12	1.584(9)
Pr1-O19	2.446(8)	P2-C17	1.838(13)	P4-C18	1.845(12)
Pr1-O11	2.450(8)	P3-O20	1.479(10)	N9-C17	1.497(15)
Pr1-O13	2.474(8)	P3-O8	1.488(9)	N9-C22	1.504(14)
Pr1-O14	2.548(1)	P3-O15	1.572(11)	N9-C18	1.500(14)
Pr1-O6	2.610(1)	P3-C22	1.850(12)		

Table S1(cont.). Selected bond distances (Å) for **Ln-H_4NMPCl**, (Ln= La, Pr, Sm, Eu, Gd, Tb, Dy and Ho) and **Ce-H_3NMP**.

[Sm(H_4NMP)(H_2O)$_2$]Cl·2H_2O					
	Length (Å)		**Length (Å)**		**Length (Å)**
Sm-O1	2.501(1)	P1-O1	1.536(5)	P3-O7	1.550(5)
Sm-O3	2.441(2)	P1-O2	1.531(5)	P3-O8	1.533(5)
Sm-O4	2.473(2)	P1-O3	1.541(5)	P3-O9	1.556(5)
Sm-O5	2.581(1)	P1-C1	1.803(5)	P3-C3	1.804(5)
Sm-O7	2.351(2)	P2-O4	1.535(5)	C1-N1	1.519(5)
Sm-O9	2.172(2)	P2-O5	1.539(5)	C2-N1	1.503(5)
Sm-Ow1	2.490(1)	P2-O6	1.532(5)	C3-N1	1.526(5)
Sm-Ow2	2.535(9)	P2-C2	1.804(5)		
[Eu(H_4NMP)(H_2O)$_2$]Cl·2H_2O					
	Length (Å)		**Length (Å)**		**Length (Å)**
Eu-O1	2.519(11)	P1-O1	1.528(4)	P3-O7	1.539(4)
Eu-O3	2.529(12)	P1-O2	1.537(4)	P3-O8	1.552(4)
Eu-O4	2.401(12)	P1-O3	1.541(4)	P3-O9	1.532(4)
Eu-O5	2.526(9)	P1-C1	1.809(4)	P3-C3	1.798(4)
Eu-O7	2.402(9)	P2-O4	1.534(1)	C1-N1	1.511(4)
Eu-O9	2.333(15)	P2-O5	1.536(4)	C2-N1	1.502(4)
Eu-Ow1	2.467(7)	P2-O6	1.538(4)	C3-N1	1.496(4)
Eu-Ow2	2.480(7)	P2-C2	1.808(4)		
[Gd(H_4NMP)(H_2O)$_2$]Cl·2H_2O					
	Length (Å)		**Length (Å)**		**Length (Å)**
Gd-O1	2.404(1)	P1-O1	1.533(4)	P3-O7	1.534(4)
Gd-O3	2.354(1)	P1-O2	1.539(4)	P3-O8	1.541(4)
Gd-O4	2.447(2)	P1-O3	1.532(4)	P3-O9	1.537(4)
Gd-O5	2.472(9)	P1-C1	1.812(4)	P3-C3	1.809(4)
Gd-O7	2.544(1)	P2-O4	1.532(4)	C1-N1	1.499(5)
Gd-O9	2.736(2)	P2-O5	1.536(4)	C2-N1	1.497(5)
Gd-Ow1	2.478(9)	P2-O6	1.541(4)	C3-N1	1.500(5)
Gd-Ow2	2.493(9)	P2-C2	1.808(4)		
[Tb(H_4NMP)(H_2O)$_2$]Cl·2H_2O					
	Length (Å)		**Length (Å)**		**Length (Å)**
Tb-O1	2.423(1)	P1-O1	1.530(4)	P3-O7	1.532(4)
Tb-O3	2.289(1)	P1-O2	1.532(4)	P3-O8	1.553(4)
Tb-O4	2.430(1)	P1-O3	1.535(4)	P3-O9	1.538(4)
Tb-O5	2.470(9)	P1-C1	1.810(4)	P3-C3	1.803(4)
Tb-O7	2.461(1)	P2-O4	1.540(4)	C1-N1	1.521(4)
Tb-O9	2.317(1)	P2-O5	1.535(4)	C2-N1	1.497(5)
Tb-Ow1	2.479(8)	P2-O6	1.540(4)	C3-N1	1.495(4)
Tb-Ow2	2.502(8)	P2-C2	1.806(4)		

Table S1 (cont.). Selected bond distances (Å) for **Ln-H_4NMPCl**, (Ln= La, Pr, Sm, Eu, Gd, Tb, Dy and Ho) and **Ce-H_3NMP**.

[Dy(H_4NMP)(H_2O)$_2$]Cl·2H_2O					
	Length (Å)		**Length (Å)**		**Length (Å)**
Dy-O1	2.418(2)	P1-O1	1.539(4)	P3-O7	1.536(4)
Dy-O3	2.389(2)	P1-O2	1.546(4)	P3-O8	1.548(4)
Dy-O4	2.332(2)	P1-O3	1.532(4)	P3-O9	1.536(4)
Dy-O5	2.407(1)	P1-C1	1.816(4)	P3-C3	1.803(4)
Dy-O7	2.353(2)	P2-O4	1.532(4)	C1-N1	1.509(4)
Dy-O9	2.321(2)	P2-O5	1.537(4)	C2-N1	1.499(5)
Dy-Ow1	2.440(9)	P2-O6	1.540(4)	C3-N1	1.488(4)
Dy-Ow2	2.459(9)	P2-C2	1.815(4)		
[Ho(H_4NMP)(H_2O)$_2$]Cl·2H_2O					
	Length (Å)		**Length (Å)**		**Length (Å)**
Ho01-O11	2.2875(2)	P1-O5	1.491(2)	P3-O11	1.493(2)
Ho01-O12	2.2967(2)	P1-O6	1.491(2)	P3-O12	1.494(2)
Ho01-O8	2.3143(2)	P1-O4	1.585(2)	P3-O10	1.570(1)
Ho01-O9	2.339(2)	P1-C1	1.841(2)	P3-C3	1.832(2)
Ho01-O6	2.3430(2)	P2-O9	1.496(2)	N1-C2	1.505(3)
Ho01-O5	2.3680(2)	P2-O8	1.510(1)	N1-C1	1.506(3)
Ho01-O2	2.3914(2)	P2-O7	1.584(2)	N1-C3	1.511(3)
Ho01-O1	2.5406(2)	P2-C2	1.817(3)		

Table S2. H-bond interactions (Å) for **[Ce_2(H_3NMP)$_2$(H_2O)$_4$]·4.5H_2O** (length < 3 Å).

Vector	**Length (Å)**	**Vector**	**Length (Å)**	**Vector**	**Length (Å)**
O1···O4	2.950(29)	O8···Ow3	2.609(33)	Ow1···Ow3	2.97(4)
O1···O10	2.831(28)	O8···Ow4	2.362(27)	Ow1···Ow6	2.50(4)
O1···Ow2	2.742(33)	O9···O18	2.290(24)	Ow1···Ow7	2.98(4)
O2···Ow2	2.671(33)	O10···O14	2.878(31)	Ow3···Ow4	2.85(4)
O2···Ow6	2.847(35)	O11···O14	2.874(32)	Ow3···Ow8	3.012(29)
O3···O15	2.478(25)	O12···Ow5	2.633(33)	Ow3···Ow9	2.724(30)
O4···O7	2.972(31)	O13···Ow3	2.882(32)	Ow4···Ow9	2.847(25)
O5···Ow4	2.922(31)	O13···O16	2.804(26)	Ow5···Ow6	2.69(4)
O5···O5	2.913(34)	O15···Ow8	2.836(19)	Ow5···Ow8	2.756(30)
O5···O8	2.758(32)	O15···Ow10	2.628(23	Ow5···Ow9	2.777(30)
O6···O17	2.330(23)	O16···Ow4	2.797(32)	Ow8···Ow10	2.47261(6)
O6···Ow6	2.74(4)	O17···Ow10	2.841(20)	Ow9···Ow10	2.87273(8)
O6···Ow7	2.786(34)	O18···Ow7	2.92(4)		
O7···O10	2.963(27)				
O7···O16	3.004(25)				

Table S3. Absorption and emission bands observed for **$[Pr(H_4NMP)(H_2O)_2]Cl \cdot 2H_2O$**.

Absorption		***Luminescence (λ_{exc} = 355 nm)***	
Transition $\leftarrow {}^3H_4$	**Wavelength (nm)**	**Transition** ${}^3P_0 \rightarrow$	**Wavelength (nm)**
$^3F_2$	1945		
$^3F_3$, $^3F_4$	1559		
$^1G_4$	1026		
$^1D_2$	592	$^3H_6$	621
$^3P_0$	481	$^3H_5$	535
$^3P_1$, $^1I_6$	469	$^3H_4$	481
$^3P_2$	444		

Table S4. Absorption and emission bands observed for **$[Sm(H_4NMP)(H_2O)_2]Cl\cdot 2H_2O$**.

Absorption		*Luminescence (λ_{exc} =355 nm)*	
Transition $\leftarrow {}^6H_{5/2}$	**Wavelength (nm)**	**Transition** ${}^4G_{5/2} \rightarrow$	**Wavelength (nm)**
$^6H_{15/2}$, $^6F_{3/2}$, $^6F_{1/2}$	1500		
$^6F_{5/2}$	1395		
$^6F_{7/2}$	1244		
$^6F_{9/2}$	1087		
$^6F_{11/2}$	948	$^6H_{9/2}$	644
$^4G_{7/2}$, $^4I_{9/2}$, $^4M_{15/2}$,	476	$^6H_{7/2}$	598
$^4I_{11/2,}$ $^4I_{13/2}$	464	$^6H_{5/2}$	562
$^4F_{5/2}$, $^4M_{17/2}$, $^4G_{9/2}$, $^4I_{15/2}$	440		
$^6P_{5/2}$	417		
$^4P_{5/2,}$ $^4F_{7/2}$, $^4F_{9/2}$, $^4K_{11/2}$, $^4M_{21/2}$, $^4L_{15/2}$, $^4G_{11/2}$	402		
$^4L_{13/2}$,	393		
$^4D_{1/2}$, $^6P_{7/2}$, $^4L_{17/2}$, $^4K_{13/2}$, $^4F_{9/2}$	374		
$^4D_{3/2}$, $^4D_{5/2}$, $^6P_{5/2}$, $^4H_{7/2}$	362		
$^4K_{15/2}$, $^4H_{9/2}$, $^4D_{7/2}$	344		

Table S5. Absorption and Emission bands observed for **[Eu(H_4NMP)(H_2O)$_2$]Cl·2H_2O**.

Absorption		*Luminescence (λ_{exc} = 355 nm)*	
Transition ← $^7F_0$	**Wavelength (nm)**	**Transition** $^5D_0$ →	**Wavelength (nm)**
$^5D_0$, $^5D_1$, $^5D_2$	**579**		
	526		
	464		
$^5L_6$	**393**	$^7F_3$	**652**
$^5G_2$, $^5G_4$, $^5G_6$	**376**	$^7F_2$	**611**
$^5D_4$	**362**	$^7F_1$	**592**
		$^7F_0$	**579**
		$^5D_1$ → $^7F_4$	**624**
		$^5L_6$ → $^7F_0$	**400**

Table S6. Absorption and emission bands observed for **[Tb(H_4NMP)(H_2O)$_2$]Cl·2H_2O**.

Absorption		*Luminescence (λ_{exc} = 355 nm)*	
Transition ← $^7F_6$	**Wavelength (nm)**	**Transition** $^5G_4$ →	**Wavelength (nm)**
$^7F_3$			
$^7F_0$, $^7F_1$, $^7F_2$	1941	$^7F_3$	620
	1446	$^7F_4$	583
$^5D_4$	487	$^7F_5$	546
	379	$^7F_6$	489
$^5G_6$, $^5D_3$, $^5L_{10}$	371		
$^5G_5$, $^5G_2$, $^5G_4$, $^5L_9$	352		
$^5D_2$, $^5L_8$, $^5L_7$, $^5G_3$	342		
$^5H_7$, $^5D_0$, $^5D_1$	318		

Table S7. Absorption and emission bands observed for **$[Dy(H_4NMP)(H_2O)_2]Cl\cdot 2H_2O$**.

Absorption		*Luminescence (λ_{ex}=355 nm)*	
Transition $\leftarrow {}^6H_{15/2}$	**Wavelength (nm)**	**Transition** ${}^4F_{9/2}\rightarrow$	**Wavelength (nm)**
$^6H_{11/2}$	1715		
$^6H_{9/2}$, $^6F_{11/2}$	1289		
$^6H_{7/2}$, $^6F_{9/2}$	1099		
$^6H_{5/2}$, $^6F_{7/2}$	907		
$^6F_{5/2}$	806	$^6H_{11/2}$	651
$^6F_{3/2}$	755	$^6H_{13/2}$	573
$^4F_{9/2}$	474	$^6H_{15/2}$	482
$^4I_{15/2}$	451		
$^4G_{11/2}$	427		
$^4M_{21/2}$, $^4I_{13/2}$, $^4F_{7/2}$, $^4K_{17/2}$, $^4M_{19/2}$	388		
$^4I_{11/2}$, $^6P_{5/2}$, $^6P_{3/2}$	364		
$^4M_{15/2}$, $^6P_{9/2}$	350		
$^4G_{9/2}$, $^4F_{5/2}$, $^4I_{9/2}$	337		
$^4K_{15/2}$, $^4L_{19/2}$, $^6P_{3/2}$, $^4M_{17/2}$, $^4G_{7/2}$	324		

Table S8. Absorption and emission bands observed for **$[Ho(H_4NMP)(H_2O)_2]Cl\cdot 2H_2O$**.

Transition $\leftarrow {}^5I_8$	Wavelength (nm)
$^5I_7$	1950
$^5I_6$	1157
$^5I_5$	896
$^5F_5$	656,643*
$^5F_4$, $^5S_2$	538
$^5F_3$	486
$^5F_2$	473
$^5F_1$	452
$^5G_5$	418
$^5G_4$	386
$^3H_6$	361
$^5G_3$,	345
$^3F_4$, $^3K_6$	332
$^3M_{10}$	305

*Shoulder